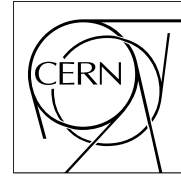


The Compact Muon Solenoid Experiment

CMS Note

Mailing address: CMS CERN, CH-1211 GENEVA 23, Switzerland



May 31, 2006

Association of jets with the signal vertex

N. Ilina, V. Gavrilov, A. Krokhotin

ITEP, Moscow, Russia

Abstract

A method for the association of jets with the signal vertex is presented. The technique is shown to reduce the instrumental background rate from jets and overlapping particles originating from additional minimum bias vertices. As a benchmark, the performance of the algorithm is evaluated using the $qq \rightarrow qqH$ search channel where the vertex assignment parameters are optimized for separating qqH and $t\bar{t}$ events. The efficiency of a central jet veto is shown to increase for the same level of background rejection. The whole study is conducted on Monte Carlo generated events that were passed through the CMS full detector-level simulation in low luminosity conditions ($L = 2 \times 10^{33} \text{ cm}^{-2} \text{ s}^{-1}$). It is shown that the method should give similar results also for high luminosity conditions ($L = 10^{34} \text{ cm}^{-2} \text{ s}^{-1}$).

1 Introduction

One of the most experimentally challenging aspects of LHC physics is the large particle multiplicities which are in part due to the presence of multiple minimum bias interactions within the same bunch crossing. The jets produced in minimum bias interactions have a sufficiently hard transverse momentum spectrum to introduce additional jets per event. Therefore, a technique to efficiently associate jets with the signal vertex is needed to reduce the large luminosity-dependent instrumental background from jets originating from additional minimum bias vertices. The CMS tracker can provide this information by associating reconstructed charged tracks to primary vertices and to jets. The idea was first proposed in [1].

To associate a jet with a vertex, a significant fraction of the tracks in the jet should originate from this vertex. In this study two separate quantities are used to quantify this fraction and their performance is compared in the analysis. The method itself was developed for the analysis of the $qq \rightarrow qqH$ search channel for different Higgs boson masses. It is essential to reject additional jets beyond the two signal jets in order to suppress $t\bar{t}$ background. Using this approach, jets which do not originate from the signal vertex are not counted as part of the jet veto. Two possibilities for determination of the signal vertex are suggested (by the muon's vertex and by the vertex with the maximum sum of corresponding tracks transverse energy). By eliminating the inefficiency of rejecting events on the basis of non-signal vertex jet, the efficiency for signal selection is increased by a factor of 2-3 for this channel.

In this note, the performance of the vertex association method is evaluated for different channels: the $qq \rightarrow qqH$, $H \rightarrow WW \rightarrow \mu\nu jj$ channel for heavy Higgs boson masses, the $qq \rightarrow qqH$, $H \rightarrow WW \rightarrow \mu\nu\mu\nu$ channel for light Higgs boson masses and QCD events.

An optimization of the algorithm parameters was performed to enhance the separation of the Higgs boson signal from the $t\bar{t}$ background. The results of this optimization are presented.

The whole study and optimization of the method are based on MC generated events that were passed through the CMS full detector-level simulation in low luminosity conditions ($L = 2 \times 10^{33} \text{ cm}^{-2}\text{s}^{-1}$). It is shown that the method should work also for high luminosity conditions ($L = 10^{34} \text{ cm}^{-2}\text{s}^{-1}$) where pile-up effects are more crucial.

All results were obtained with the data generated by PYTHIA 6.214 generator [2], the CMS full detector simulation and reconstruction was done with simulation package OSCAR 245[3] and with the CMS object-oriented reconstruction package ORCA version 7.6.1 [4].

The analysis of the reconstructed events was done with ORCA version 8.7.4[4].

2 Description of the method

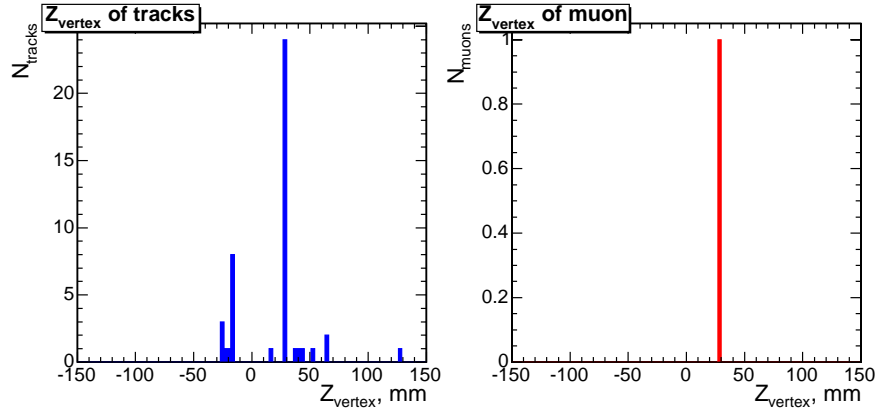
In this section plots for low luminosity conditions ($L = 2 \times 10^{33} \text{ cm}^{-2}\text{s}^{-1}$) are shown for $qq \rightarrow qqH$, $H \rightarrow WW \rightarrow l\nu jj$ events with $M_H = 600 \text{ GeV}/c^2$. A sample of 12000 events was analyzed.

The plots for high luminosity conditions ($L = 10^{34} \text{ cm}^{-2}\text{s}^{-1}$) are given for $qq \rightarrow qqH$, $H \rightarrow WW \rightarrow l\nu jj$ events with $M_H = 500 \text{ GeV}/c^2$. A sample of 3000 events was analyzed.

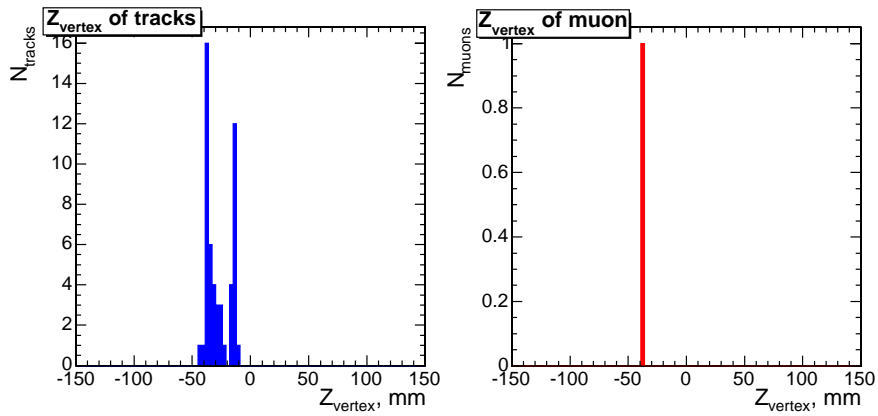
2.1 Determination of the signal vertex by muon's vertex in the event

The tracking reconstruction provides a list of tracks per event. Each reconstructed track is assigned an impact parameter along the Z axis (Z_{vertex}).

In the $H \rightarrow WW \rightarrow \mu\nu jj$ decay, the muon Z_{vertex} determines the location of the signal vertex. In Fig.1 the distributions of the Z_{vertex} for all charged particle tracks (left plot) and muons (right plot) are shown for two particular events (a,b), simulated in low luminosity conditions.



a)

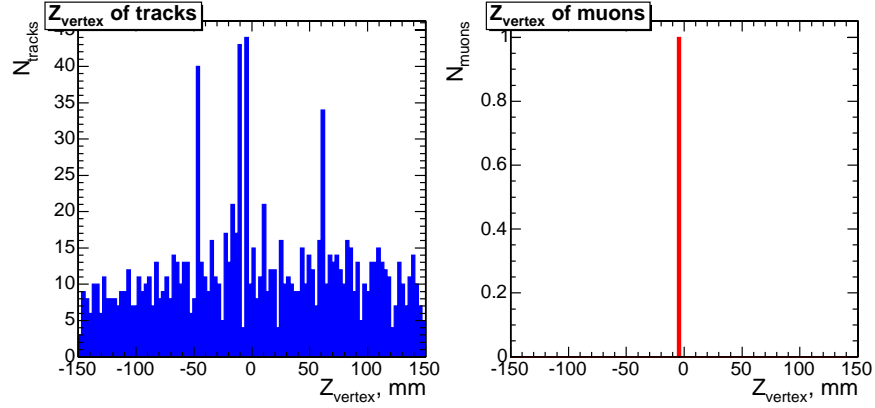


b)

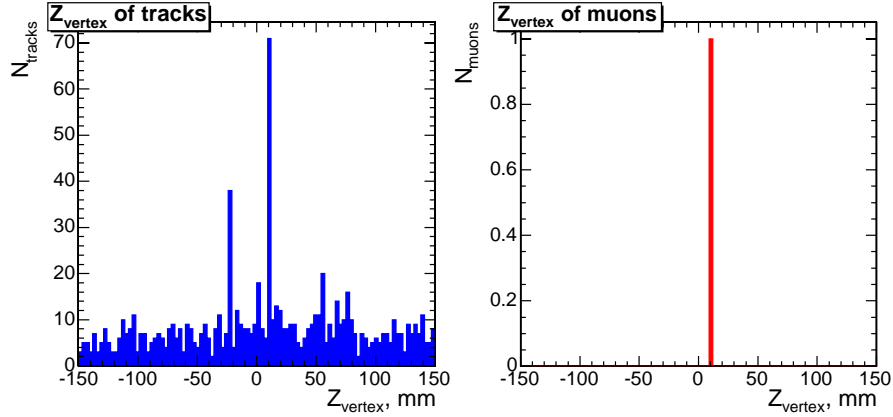
Figure 1 (a, b): The distribution of the Z_{vertex} of all charged particle tracks (left plot) and of muons (right plot) in two particular events at low luminosity.

Several peaks appear in the left plot for each event, but only one peak corresponds to the signal vertex. The muon Z_{vertex} is used to define the signal vertex.

The same distributions for high luminosity conditions are shown in Fig.2(a, b). There are much more tracks originating from additional minimum bias vertices. But the signal vertex could be defined, however, by the reconstructed vertex of the muon.



a)



b)

Figure 2 (a, b): The distribution of the Z_{vertex} of all charged particle tracks (left plot) and of muons (right plot) in two particular events at high luminosity.

2.2 Procedure for the identification of the jets from the signal vertex

There are two approaches to test whether jets originate from the signal vertex or not. They differ in the use of the calorimeter jet energy measurement.

Method A:

1) The variable α_{jet} is determined for each jet as the ratio of the sum of transverse momenta of all tracks found inside the jet cone and having the same vertex as the signal muon to the transverse momentum of the jet as measured by the calorimeters,

$$\alpha_{\text{jet}} = \frac{\sum P_T^{\text{track}_\alpha}}{P_T^{\text{jet}}} .$$

A track is considered to have the same vertex as the muon if $|Z_{\text{vertex}}^{\text{track}} - Z_{\text{vertex}}^{\mu}| < dZ$.

- 2) If $\alpha_{\text{jet}} > \alpha_0$, this jet is assigned to the signal vertex.

Method B:

1) The variable β_{jet} is determined for each jet as the ratio of the sum of transverse momenta of all tracks found inside the jet cone and having the same vertex as the signal muon to the transverse momentum of all tracks inside the jet cone,

$$\beta_{\text{jet}} = \frac{\sum P_T^{\text{track}_\alpha}}{\sum P_T^{\text{track}}}$$

A track is considered to have the same vertex as the muon if $|Z_{\text{vertex}}^{\text{track}} - Z_{\text{vertex}}^{\mu}| < dZ$.

- 2) If $\beta_{\text{jet}} > \beta_0$, this jet is assigned to the signal vertex.

The parameters of this procedure are dZ and $\alpha_0(\beta_0)$.

The distribution on the Z_{vertex} difference between the tracks and the muon is shown in Fig.3 for low luminosity and Fig.4 for high luminosity. The value of $dZ = 1\text{mm}$ was chosen.

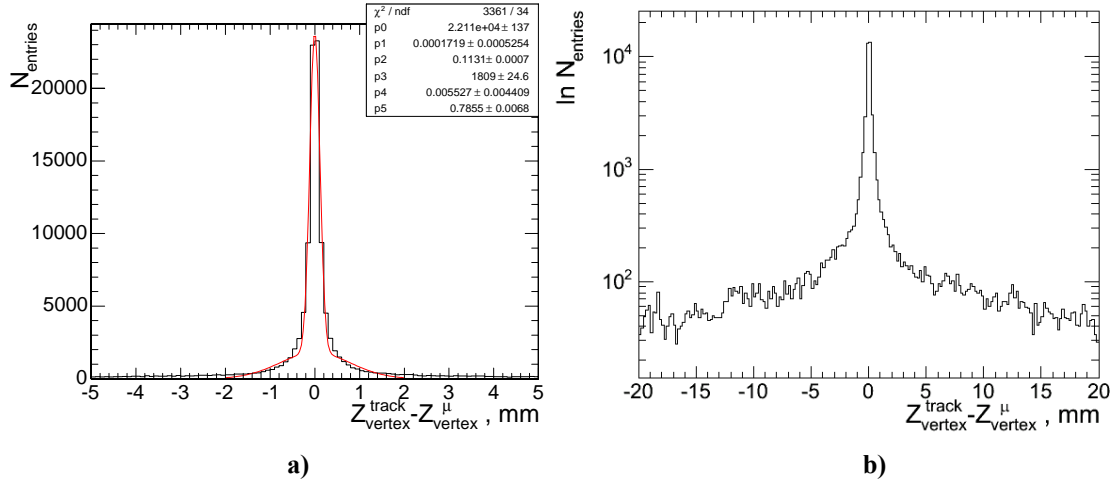


Figure 3: Distribution of the Z_{vertex} difference between the tracks and the muon at low luminosity:

a) linear scale b) logarithmic scale

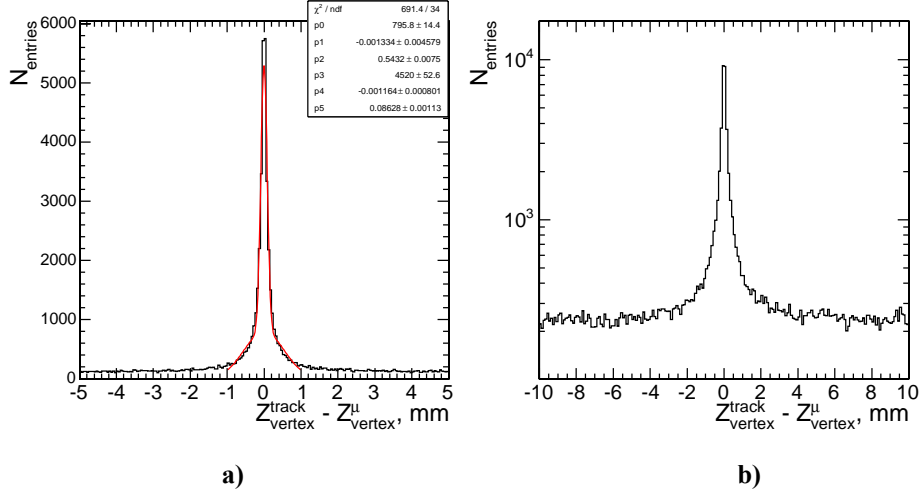


Figure 4: Distribution of the Z_{vertex} difference between the tracks and the muon at high luminosity:
a) linear scale b) logarithmic scale

2.3 Determination of the signal vertex without muon in the event

Another possibility for determination of the signal vertex is suggested. One can calculate for every vertex the sum of transverse energy for all tracks originating from this vertex. After that the vertex with the maximum sum should be determined as the signal vertex in the event.

The distribution on the Z_{vertex} difference between the tracks and the signal vertex defined by this way is shown in Fig.5. This plot was obtained by analysis of QCD events at low luminosity.

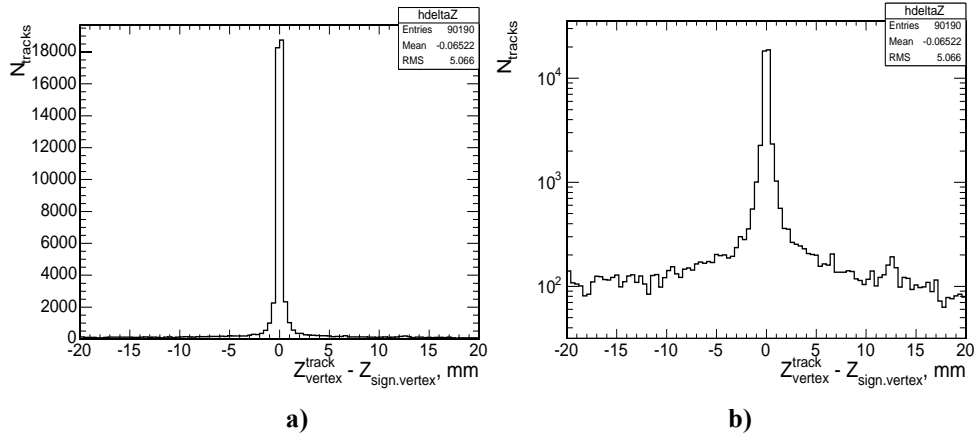


Figure 5: Distribution of the Z_{vertex} difference between the tracks and the signal vertex defined by the maximum $\sum P_T$ of tracks: a) linear scale b) logarithmic scale

3 Application of the method: the central jet veto for $qq \rightarrow qqH$ channels

Two different $qq \rightarrow qqH$ channels: $H \rightarrow WW \rightarrow \mu\nu jj$ ($M_H = 600 \text{ GeV}/c^2$) and $H \rightarrow WW \rightarrow \mu\nu\mu\nu$ ($M_H = 150 \text{ GeV}/c^2$) were studied in low luminosity conditions.

In the $qq \rightarrow qqH, H \rightarrow WW \rightarrow \mu\nu jj$ channel ($M_H = 600 \text{ GeV}/c^2$) the signal efficiencies from the full detector simulation and from a simplified particle-level simulation were compared. The set of selection criteria for this channel was developed in [5,6] and the results are summarized in Appendix A. The signal efficiencies are in reasonable agreement for all selection criteria except for the central jet veto. The central jet veto is the requirement that there are no additional jets found in the event in the central rapidity region of the detector. For particle-level analyses, this requirement was found to be effective in rejecting $t\bar{t}$ background while maintaining high efficiency for the signal. However, with the full detector simulation the signal efficiency decreases: from 80% at the particle level to 26% with the calorimetric-based central jet veto criterion. One of the reasons for this difference is the signal contamination by jets with low transverse energy coming from minimum bias events.

In order to eliminate these jets the vertex association method described above was used, and the central jet veto was applied only to jets identified as coming from the signal vertex.

In total a sample of 12000 events with an electron or a muon in final state were analyzed. Jets were reconstructed with the Iterative Cone Algorithm[3]. The parameters of this algorithm were chosen as follows: cone size for jets = 0.5, seed cut = 2.0 GeV, jet threshold = 10 GeV. The MC jet correction coefficients for cone size 0.5 HLT jets at low luminosity were used. The veto threshold was $P_T^{\text{threshold}} > 20\text{GeV}$ and $\alpha = 0.3$ for the veto algorithm using jet vertex assignment.

As a result the signal selection efficiency increased from 26% to 56%.

For high luminosity conditions the result is expected to be more pronounced due to the huge background from additional minimum bias interactions (as it was shown in Section 2.1). But for the moment there is no possibility to make the quantitative analysis because the jet energy corrections and corrections for missing energy haven't done yet for high luminosity.

The vertex assignment method was also applied to the $qq \rightarrow qqH, H \rightarrow WW \rightarrow \mu\nu\mu\nu$ channel ($M_H = 150 \text{ GeV}/c^2$). A sample of 5064 events at low luminosity was used in the analysis. Jets were reconstructed and correction coefficients applied as it was described for $qq \rightarrow qqH, H \rightarrow WW \rightarrow \mu\nu jj$ channel. The set of selection criteria for this channel was developed in references [7,8], see Appendix B. These criteria were applied as they are except the value of $P_T^{\text{threshold}}$. It was optimized together with the parameter α using sample of $t\bar{t}$ events with full detector simulation as it's described in section 4 of this note. It was found that optimal parameters are $P_T^{\text{threshold}} > 30\text{GeV}$ and $\alpha = 0.2$. Using this criteria a signal efficiency of 90% can be achieved while maintaining background rejection at the appropriate level.

Such kind of optimization was not possible for $qq \rightarrow qqH, H \rightarrow WW \rightarrow \mu\nu jj$ channel ($M_H = 600 \text{ GeV}/c^2$). Because of the more strict selection criteria used for the analysis of this channel the number of $t\bar{t}$ events after application of all the criteria except central jet veto becomes small that makes further optimization not possible.

4 Optimization of the algorithm parameters

The optimization of the parameters was done by comparing signal efficiency and background rejection. The channel $qq \rightarrow qqH, H \rightarrow WW \rightarrow \mu\nu\mu\nu$ ($M_H = 150 \text{ GeV}/c^2$) was chosen to be the signal, and the background consist of $t\bar{t}$ events with at least one muon in the final state. A sample of 51150 $t\bar{t}$ events at low luminosity was used.

The method of jet association with the signal vertex was utilized for both signal and $t\bar{t}$ samples. The central jet veto was applied only for jets identified as coming from the signal vertex.

Fig.6 shows the fraction of $t\bar{t}$ events passing the central jet veto divided by fraction of signal events passing central jet veto vs. the fraction of signal events passing central jet veto. The different curves correspond to different values of the parameter α . Each curve has been drawn through the set of six points corresponding to the different values of $P_T^{\text{threshold}}$ used in the central jet veto. The values of $P_T^{\text{threshold}}$ from left to right are 20 GeV, 25 GeV, 30 GeV, 35 GeV, 40 GeV and 45 GeV. The curve for $\alpha=0$ which

corresponds to the case of no vertex assignment was drawn through the set three points corresponding to the values of $P_T^{\text{threshold}}$: 20GeV, 25GeV, 30GeV.

Fig.7 is the same as Fig.6 but for the parameter β .

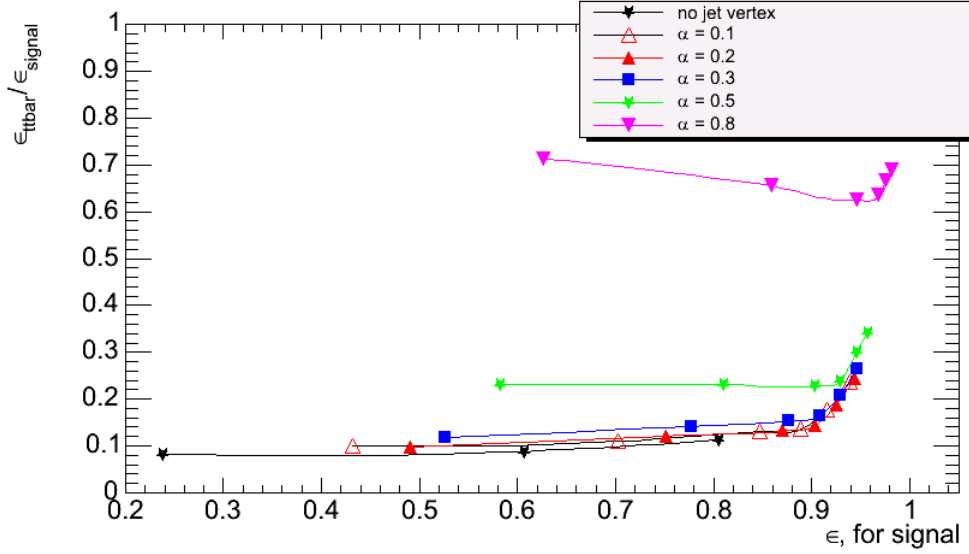


Figure 6: Fraction of background events passing the central jet veto divided by the same fraction for signal events vs. fraction of signal events passing central jet veto for different values of parameter α .

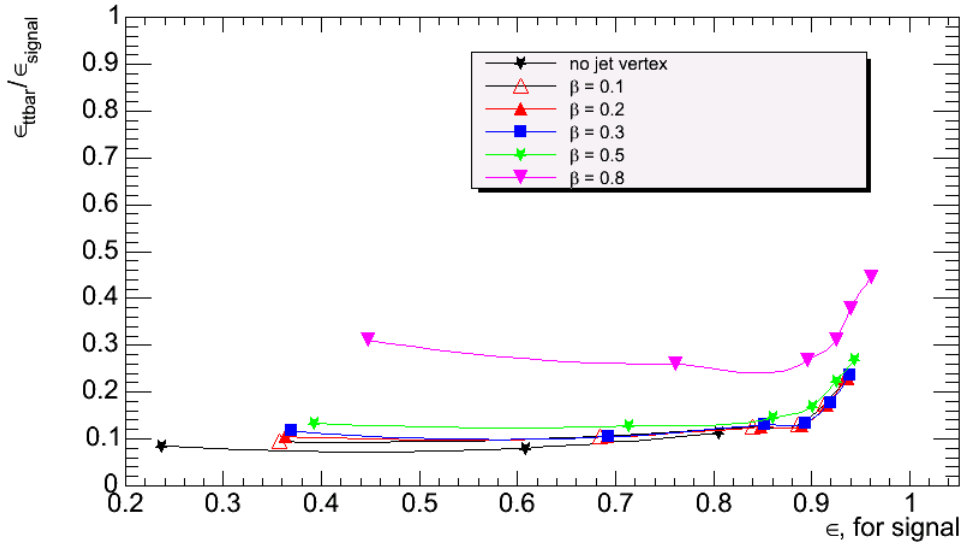


Figure 7: Fraction of background events passing the central jet veto divided by the same fraction for signal events vs. fraction of signal events passing central jet veto for different values of parameter β .

The lowest curves on these figures (at $\alpha = 0.2$ and $\beta = 0.2$) can be considered as optimal. Reducing these parameters further has no visible effect. The best operation point corresponds to $P_T^{\text{threshold}} = 30$ GeV. This point gives the best efficiency of the central jet veto: the efficiency of jet veto for signal is quite high while the ratio between background and signal efficiencies is still small.

In Fig.8(9) the efficiency of central jet veto for the signal and $t\bar{t}$ vs. $P_T^{\text{threshold}}$ is shown for $\alpha(\beta) = 0.2$.

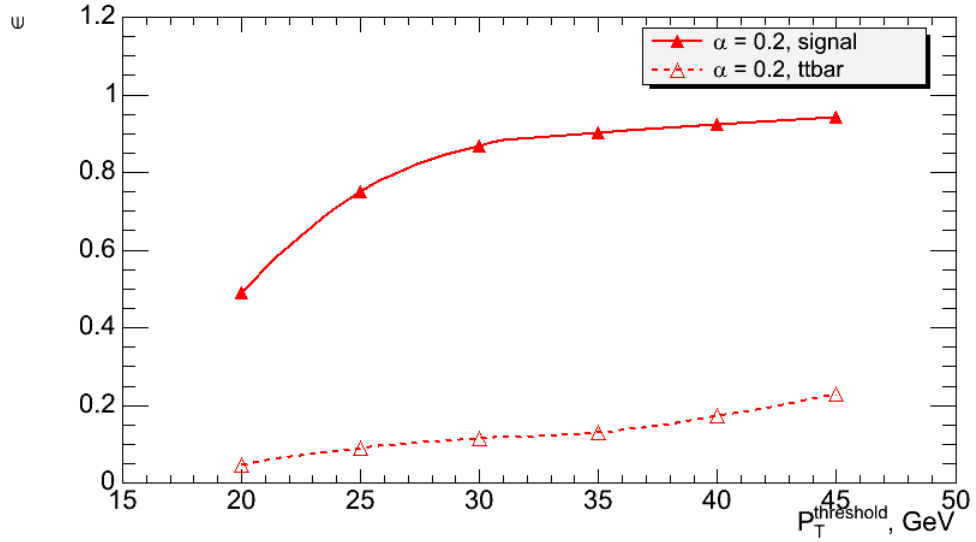


Figure 8: The efficiency of the central jet veto for the signal vs. $P_T^{\text{threshold}}$ for $\alpha = 0.2$.

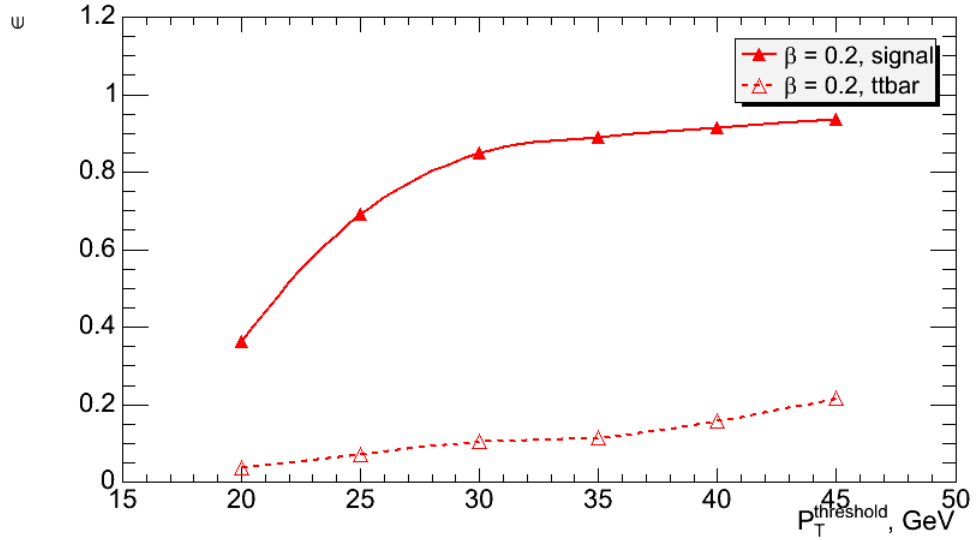


Figure 9: The efficiency of the central jet veto for the signal vs. $P_T^{\text{threshold}}$ for $\beta = 0.2$.

5 Summary

A method of associating jets with the signal vertex was presented. By using tracking information to assign jets to their corresponding vertex, instrumental backgrounds from jets from minimum bias interactions can be suppressed.

This method was applied to different $qq \rightarrow qqH$ channels: $H \rightarrow WW \rightarrow \mu\nu jj$ ($M_H = 600 \text{ GeV}/c^2$) and $H \rightarrow WW \rightarrow \mu\nu\mu\nu$ ($M_H = 150 \text{ GeV}/c^2$) at low luminosity conditions. One of the important selection criteria for these channels, the central jet veto, was modified to reject only those additional jets originating from the

signal vertex as determined by the vertex association method. The implementation of the vertex association method substantially improves the signal selection efficiency.

The optimization of the algorithm parameters was done by comparing the signal efficiency versus $t\bar{t}$ background rejection. It was shown that the best choice of the parameters is $dZ = 1\text{mm}$ and $\alpha_0(\beta_0) = 0.2$. For the signal channel, the value of $P_T^{\text{threshold}} = 30\text{ GeV}$ for central jet veto gave the best results. These parameters give a high level of background suppression while keeping 90% signal efficiency.

For high luminosity conditions the method should work also. It was shown that the background from minimum bias interactions was more important but it was possible to determine the signal vertex.

Appendix A

The set of cuts for the $qq \rightarrow qqH$, $H \rightarrow WW \rightarrow \mu\nu jj$ channel ($M_H = 600\text{ GeV}/c^2$):

I. Cuts on the muon: $|\eta_\mu| < 2.4$, $P_T^\mu > 30\text{ GeV}$. The muon with the highest transverse momentum is chosen in events with multiple muons.

II. Cuts on the W boson that decays to muon and neutrino ($W \rightarrow \mu\nu$):

$$E_T^{\text{miss}} > 30\text{ GeV}, M_T^{W \rightarrow \mu\nu} < 100\text{ GeV}/c^2, P_T^{W \rightarrow \mu\nu} > 250\text{ GeV}/c;$$

where $P_T^{W \rightarrow \mu\nu}$ and $M_T^{W \rightarrow \mu\nu}$ are calculated from components of E_T^{miss} and P_T^μ using

$$P_T^{W \rightarrow \mu\nu} = \sqrt{(P_T^\mu + E_T^{\text{miss}})_X^2 + (P_T^\mu + E_T^{\text{miss}})_Y^2}, M_T^{W \rightarrow \mu\nu} = \sqrt{(P_T^\mu)^2 + (E_T^{\text{miss}})^2 - (P_T^{W \rightarrow \mu\nu})^2}$$

III. Cuts on the W boson that decays to jets ($W \rightarrow jj$):

$$|\eta_j| < 3, P_T^j > 40\text{ GeV}/c, P_T^{W \rightarrow jj} > 250\text{ GeV}/c, 60\text{ GeV}/c^2 < M^{W \rightarrow jj} < 100\text{ GeV}/c^2,$$

jet pair with the largest transverse momentum is chosen.

IV. Cuts on tagging jets:

$$\text{two jets } (j_1, j_2) \text{ are identified to be tagging jets if } P_T^{j_1, j_2} > 20\text{ GeV}/c, \eta_{j_1} \cdot \eta_{j_2} < 0,$$

$$|\eta_{j_1} - \eta_{j_2}| > 4, P_T^{j_1, j_2} > 300\text{ GeV}/c$$

V. Central jet veto:

there must be no additional central jets ($|\eta| < 2.5$) with $P_T^j > P_T^{\text{threshold}} = 20\text{ GeV}/c$ other than the two jets from W decay and possibly one or two tagging jets (if they are in the $|\eta| < 2.5$ region).

Appendix B

The set of cuts for the $qq \rightarrow qqH$, $H \rightarrow WW \rightarrow \mu\nu\mu\nu$ channel ($M_H = 150\text{ GeV}/c^2$):

I. Cuts on tagging jets:

$$\text{two jets } (j_1, j_2) \text{ are identified to be tagging jets if } P_T^{j_1, j_2} > 20\text{ GeV}/c, \eta_{j_1} \cdot \eta_{j_2} < 0,$$

$$|\eta_{j_1} - \eta_{j_2}| > 4, \Delta R_{j_1 j_2} > 0.6, m_{j_1 j_2} > 600\text{ GeV}/c^2.$$

II. Cuts on muons:

$$|\eta_\mu| < 2.5, P_T^\mu > 20, 10\text{ GeV}/c, \eta_{j_1} + 0.6 < \eta_\mu < \eta_{j_2} - 0.6, m_{\mu\mu} < 60\text{ GeV}/c^2, \phi_{\mu\mu} < 140^\circ.$$

$$\Delta R_{j1} > 0.7$$

III. Central jet veto:

there must be no additional central jets with $P_T^j > P_T^{\text{threshold}} = 20 \text{ GeV}/c$ in the region $\eta_{j1} + 0.5 < \eta_j < \eta_{j2} - 0.5$.

6 Acknowledgements

We would like to thank Alexander Nikitenko, James Rolf and Chris Tully for their comments and suggestions.

This work was partly supported by INTAS YSF 05-112-5263.

References

- [1] V.Drollinger, T.Muller, D.Denegri, Prospects for Higgs Boson Searches in the Channel $WH \rightarrow lvbb$, CMS NOTE-2002/006;
- [2] T.Sjostrand, L.Lonnblad and S.Mrenna, arXiv:hep-ph/0108264;
- [3] CMS Collaboration, Object-oriented Simulation for CMS Analysis and Reconstruction, Physics TDR Vol.I, Chapter2; <http://cmsdoc.cern.ch/oscar>;
- [4] CMS Collaboration, *CMS OO Reconstruction*, Physics TDR Vol.I, Chapter2; <http://cmsdoc.cern.ch/orca> ;
- [5] S. Abdullin, N. Stepanov, Search or heavy HIGGS via the $H \rightarrow lvjj$ and $H \rightarrow lljj$ channels, CMS TN-1993/088;
- [6] S. Abdullin, N. Stepanov, Towards self-consistent scenario of the heavy higgs observability via the channel $lvjj$ at CMS, CMS TN-1994/178;
- [7] N.Kauer, T.Plehn, D.Rainwater, D.Zeppenfeld, Physics Letters B 503(2001);
- [8] N.Akchurin, D.Green, S.Kunori, R.Vidal, W.Wu, M.T.Zeyrek CMS NOTE 2002/01.